Article

Molecular editing of aza-arene C–H bonds by distance, geometry and chirality

https://doi.org/10.1038/s41586-022-05175-1

Received: 17 August 2021

Accepted: 2 August 2022

Published online: 9 August 2022

Check for updates

Zhoulong Fan[1,3], Xiangyang Chen[2,3], Keita Tanaka[1], Han Seul Park[1], Nelson Y. S. Lam[1], Jonathan J. Wong[2], K. N. Houk[2]✉ & Jin-Quan Yu[1]✉

Direct molecular editing of heteroarene carbon–hydrogen (C–H) bonds through consecutive selective C–H functionalization has the potential to grant rapid access into diverse chemical spaces, which is a valuable but often challenging venture to achieve in medicinal chemistry[1]. In contrast to electronically biased heterocyclic C–H bonds[2–9], remote benzocyclic C–H bonds on bicyclic aza-arenes are especially difficult to differentiate because of the lack of intrinsic steric/electronic biases[10–12]. Here we report two conceptually distinct directing templates that enable the modular differentiation and functionalization of adjacent remote (C6 versus C7) and positionally similar (C3 versus C7) positions on bicyclic aza-arenes through careful modulation of distance, geometry and previously unconsidered chirality in template design. This strategy enables direct C–H olefination, alkynylation and allylation at adjacent C6 and C7 positions of quinolines in the presence of a competing C3 position that is spatially similar to C7. Notably, such site-selective, iterative and late-stage C–H editing of quinoline-containing pharmacophores can be performed in a modular fashion in different orders to suit bespoke synthetic applications. This Article, in combination with previously reported complementary methods, now fully establishes a unified late-stage 'molecular editing' strategy to directly modify bicyclic aza-arenes at any given site in different orders.

The efficient generation of diverse analogues with structural modifications at various sites presents a continuing synthetic challenge that underpins drug discovery. For a given molecular scaffold or pharmacophore, the selective and iterative activation of multiple inert carbon–hydrogen (C–H) bonds at different sites represents the most direct strategy for the rapid and efficient generation of structural diversity[1,13]. For example, functionalization with ten coupling partners at five different sites of a quinoline scaffold could rapidly generate up to 100,000 structurally unique analogues using a unified editing strategy (Fig. 1a). This notionally ideal 'molecular editing' approach, however, is marred by a lack of reliable methods for late-stage selective functionalization of pharmacophores, curtailing broader realization in a translational context[14,15]. As privileged pharmacophores for diverse biological targets, aza-arene heterocycles are particularly dominant within the realm of drug discovery. Within the azine component, leveraging a substrate's intrinsic electronic properties has enabled the now-established site-selective functionalizations of C2–H[3,4] and C4–H[5,6,8,9] under a nucleophilic metallation regimen, and at C3–H[2,7] through the corresponding electrophilic metallation process. By contrast, selective functionalization of multiple C–H bonds on the benzocyclic component of bicyclic aza-arene heterocycles remains to be realized. For these chemically similar C–H bonds, leverage of proximity-driven effects to selectively direct the catalyst has been limited to benzocyclic C8–H bonds adjacent to Lewis basic heteroatoms[10–12]. Notably, the selective editing of remote positions, such as C5–C7 on quinoline-type scaffolds, remains inaccessible to the established electronically driven or substrate-directed approaches described above (Fig. 1a).

We surmised that this eminent problem could be solved using reversibly binding directing templates capable of selectively positioning the catalyst proximate to a target remote C–H bond through a macrocyclophanic pretransition state[16–20]. In this context, bicyclic aza-arene scaffolds pose further obstacles for template-directed remote regioselection; in addition to suppressing functionalization at activated sites (C2–C4), the multiple adjacent yet minutely inequivalent and unactivated remote benzocyclic positions (C5–C7) demand stringent regiochemical precision for their discrimination and selective activation. The feasibility of this template-directed approach for the activation of remote benzocyclic C–H bonds was first indicated in 2017, when stoichiometric template loadings to overcome deleterious azine binding enabled the singular C5–H palladation and functionalization of quinoline[21,22]. In combination with norbornene relay, an indirect C6-selective arylation can also be realized on the basis of this C5–H palladation, although this strategy only permits arylation with electron-deficient aryl iodides, requires a vacant C5 position and fundamentally does not provide a solution for the selective C6–H palladation and diverse functionalization necessary to achieve molecular editing[23]. The direct activation of C6 and C7 positions, as compared with the marginally more nucleophilic C5 and C8 positions, is particularly difficult both for the chemical inertness and electronic similarity of the two C–H bonds. Careful spatial analysis revealed subtle differences between

[1]Department of Chemistry, The Scripps Research Institute, La Jolla, CA, USA. [2]Department of Chemistry and Biochemistry, University of California, Los Angeles, CA, USA. [3]These authors contributed equally: Zhoulong Fan, Xiangyang Chen. ✉e-mail: houk@chem.ucla.edu; yu200@scripps.edu

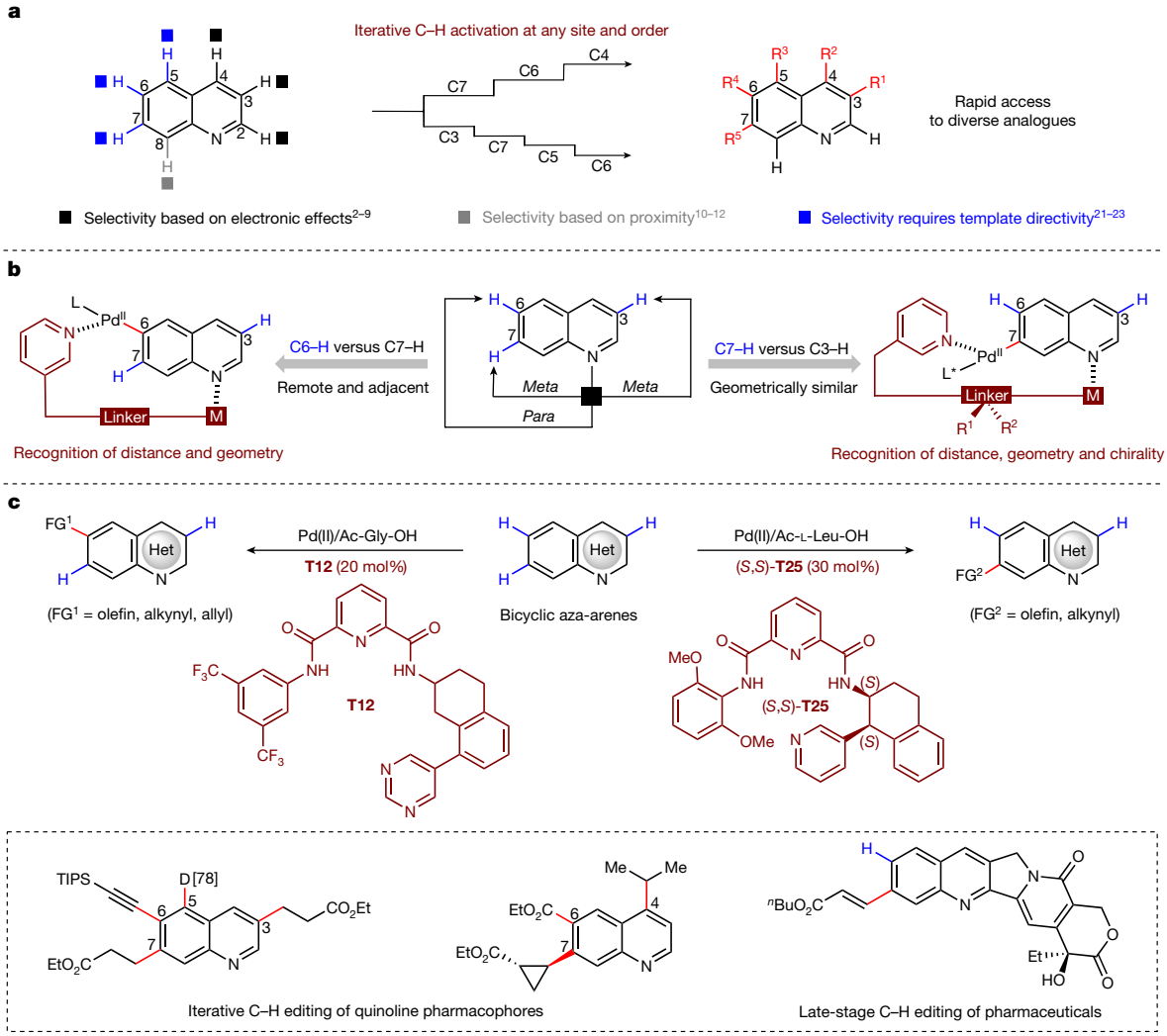

Fig. 1 | Molecular editing of heterocycles. a, Molecular editing of quinoline. **b**, Challenges and solutions to C6- and C7-selective palladation. **c**, Catalytic C6- and C7-selective functionalizations (this work). M, metal; L, ligand; FG, functional group; TIPS, triisopropylsilyl; ^{n}Bu, *n*-butyl.

C6–H and C7–H in both distance (one bond difference) and geometry (*meta* versus *para*), suggesting the possibility of precise template design to differentiate between these two C–H bonds. The same analysis also revealed that the sterically similar and more activated C3–H possesses a similar distance (one bond difference) but identical geometry (*meta* versus *meta*) to our desired C7–H bond. The latter challenge suggested that judicious spatial tuning of template distance and two-dimensional geometry may not be sufficient to impart selectivity for the remote C7 position. To address these pitfalls, we were further inspired by chiral catalyst-controlled regioselective functionalization of chiral polyols[24–26]. This led to the design of a chiral template, which upon interaction with a matched chiral catalyst, is capable of distinguishing between C3–H and C7–H positions thereby providing the desired C7-selective functionalization (Fig. 1b).

Here we report two conceptually distinct directing templates that enable site-selective C6–H and C7–H activation of bicyclic aza-arenes. These catalytic pyridine-based templates recruit the aza-arene substrate through *N*-coordination, enabling the directing arm to deliver the catalyst and precisely activate remote and adjacent C6–H or C7–H bonds (Fig. 1c). In parallel, we found that the use of a simple and readily prepared template chaperone (**TC**) can turn over the directing template, enabling it to be used catalytically (Supplementary Information Section 2.3). Notably, chiral recognition is vital in the granular discrimination between competing C3–H and C7–H bonds when differentiation by distance and geometry is insufficient. Thus, precise spatial and chiral recognition of a directing template now enables the iterative C–H editing of quinoline pharmacophores at any desired site and order.

Using quinoline **1a** as the model substrate, we initially targeted the development of a selective C6–H olefination reaction. Considering that our previous C5 template is used in stoichiometric amounts, a key objective at the outset of our studies was the catalytic use of our templates. This was solved by an easily synthetized symmetrical template chaperone **TC8** (two steps, no chromatography) to mask the quinoline nitrogen and facilitate product turnover from the directing template. An initial hit was found through a systematic screen of linker length in the presence of 2-fluoro-3-phenylpyridyl motif as the directing group (**T3**, Supplementary Table 1)[27]. A rigidified analogue of **T3** bearing an alicyclic two-carbon spacer (**T8**) was next pursued, which gave a marked improvement to both yield and C6 selectivity. Further tuning of the directing motif (**T9** to **T12**, Supplementary Table 1) showed that yields were improved using 3-phenylpyrimidyl-bearing **T12** (Fig. 2a), whereas an assessment of the left-hand portion of the template and template chaperone scaffolds gave no noticeable improvements in reactivity and selectivity. The optimal result with **T12** and **TC8**, both bearing 3,5-ditrifluoromethylphenyl side arms, probably arises from their structural homology, improving the efficacy of substrate–product exchange in the reaction. In all cases, the incorporated palladium within the directing template and template chaperones can be easily

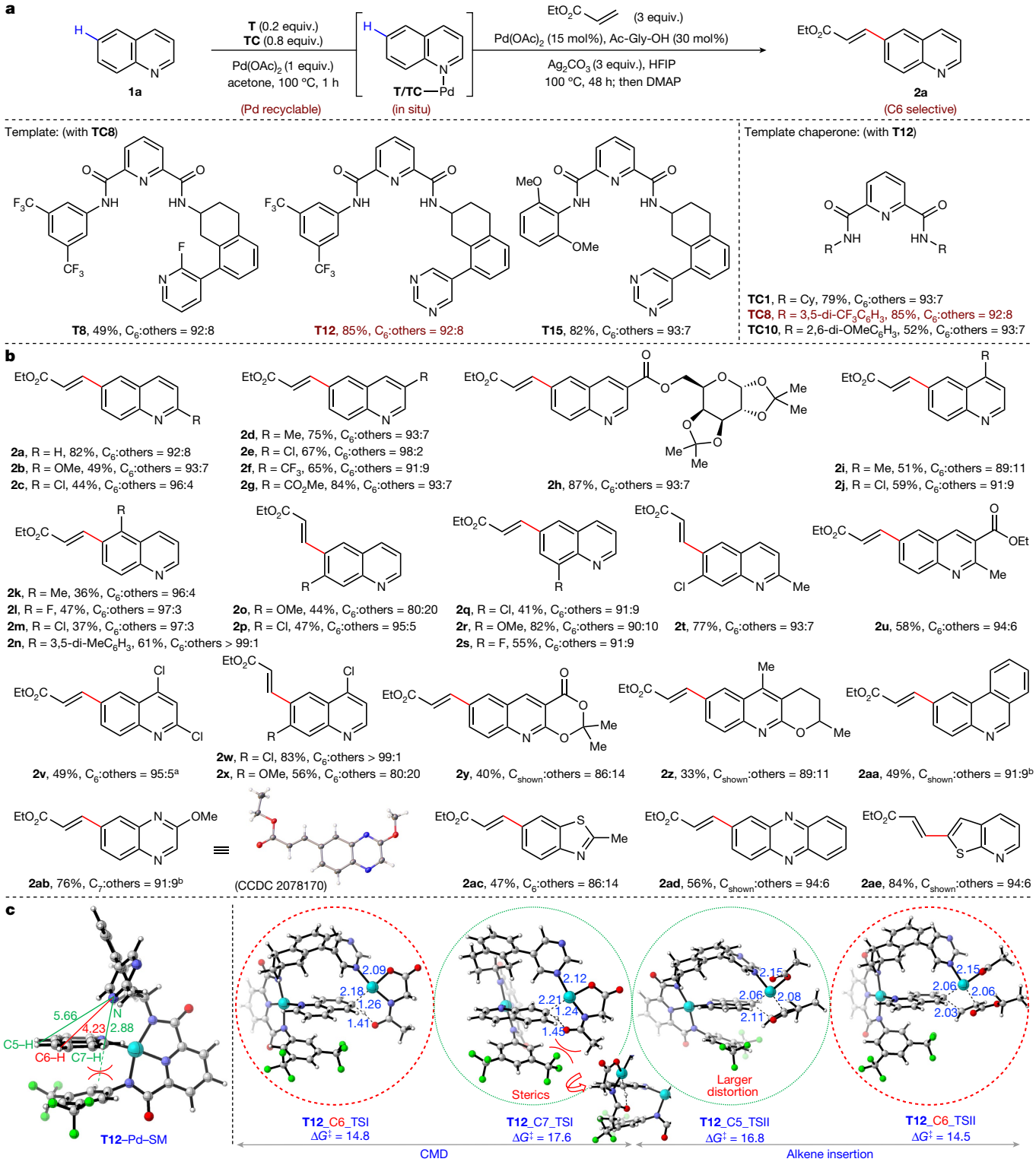

Fig. 2 | C6 (and related)-selective C–H olefination reactions of quinoline and other heterocycles. a, Selected optimization of the directing template and template chaperone scaffolds. **b**, The scope of aza-arenes. **c**, DFT analysis rationalizes the observed C6 selectivity of quinoline **1a** for template **T12**. Optimization yield and selectivity of **2a** are determined by ^{1}H NMR analysis. All yields are isolated yields for reaction scope. Bond lengths are denoted in angstroms. All energies are in kcal mol^{-1}. [a]Using **T8** (0.2 equiv.). [b]Using **T15** (0.2 equiv.) and **TC10** (0.8 equiv.). Cy, cyclohexyl; DMAP, 4-(dimethylamino) pyridine; HFIP, 1,1,1,3,3,3-hexafluoro-2-propanol; SM, starting material; TS, transition state.

recovered as the **TC**–Pd–MeCN complex, and recycled with no loss in reaction efficacy (Supplementary Information section 2.9).

With optimized template and conditions in hand, we next evaluated the reaction scope with respect to quinoline and related heterocycles (**2a** to **2ae**, Fig. 2b). Various electron-donating and electron-withdrawing groups were compatible in the reaction, showing little difference in yield or selectivity (**2a** to **2s**), confirming the power of our proximity-driven directing approach in overriding inherent

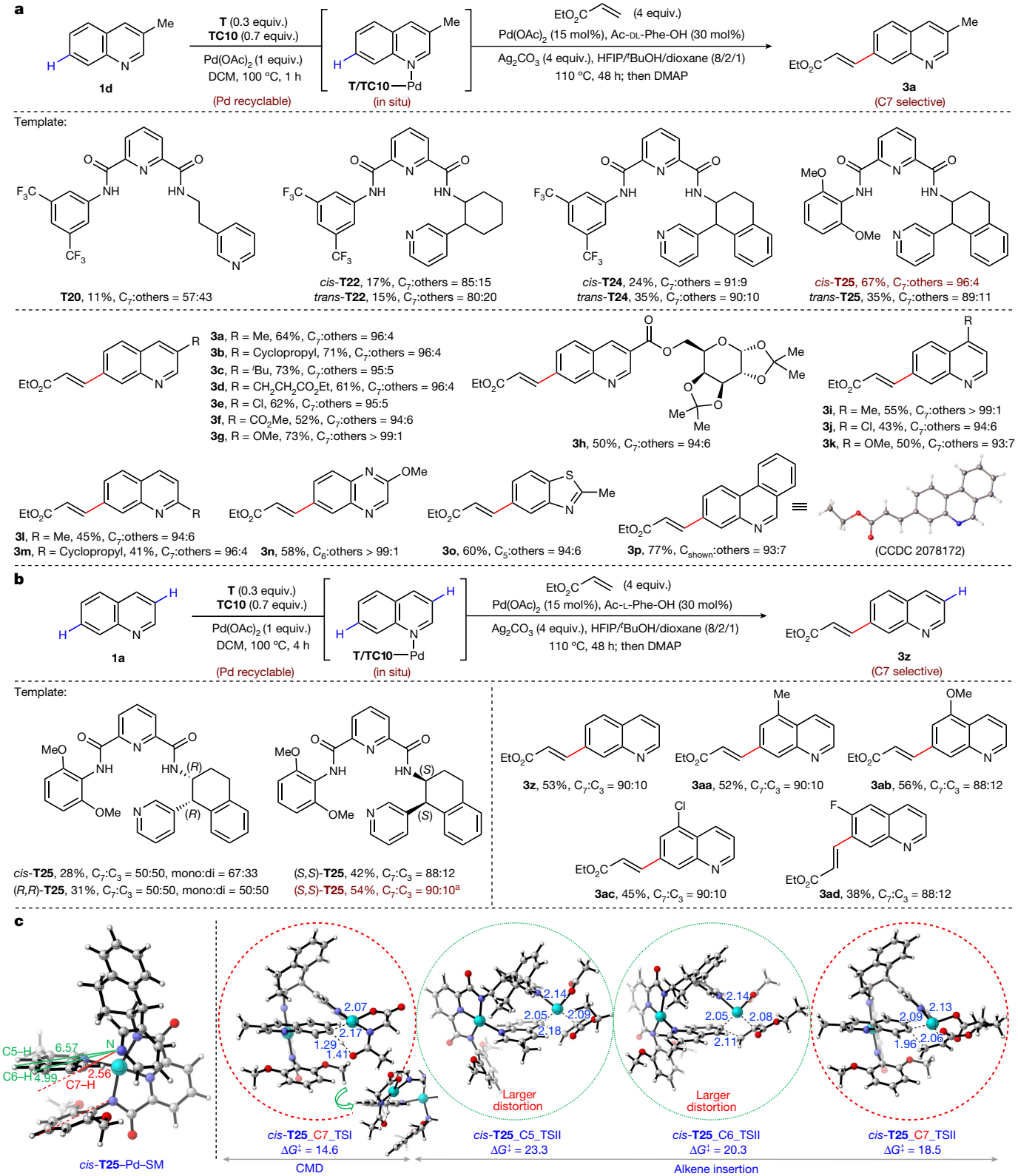

Fig. 3 | C7 (and related)-selective C–H olefination reactions of quinoline and other heterocycles. a, Selected template optimization for C7 olefination of **1d** and the scope of heterocyclic substituted substrates. **b**, Selected condition optimization for C7 olefination of **1a** and the scope of benzocyclic substituted substrates. **c**, DFT analysis rationalizes the observed C7 selectivity of 3-methylquinoline **1d** for template *cis*-**T25**. Optimization yield and selectivity are determined by ^{1}H NMR analysis. All yields are isolated yields for reaction scope. Bond lengths are denoted in angstroms. All energies are in kcal mol^{-1}. [a]Using $Pd(MeCN)_2Cl_2$ (15 mol%) and Ac-L-Leu-OH (30 mol%). DCM, dichloromethane.

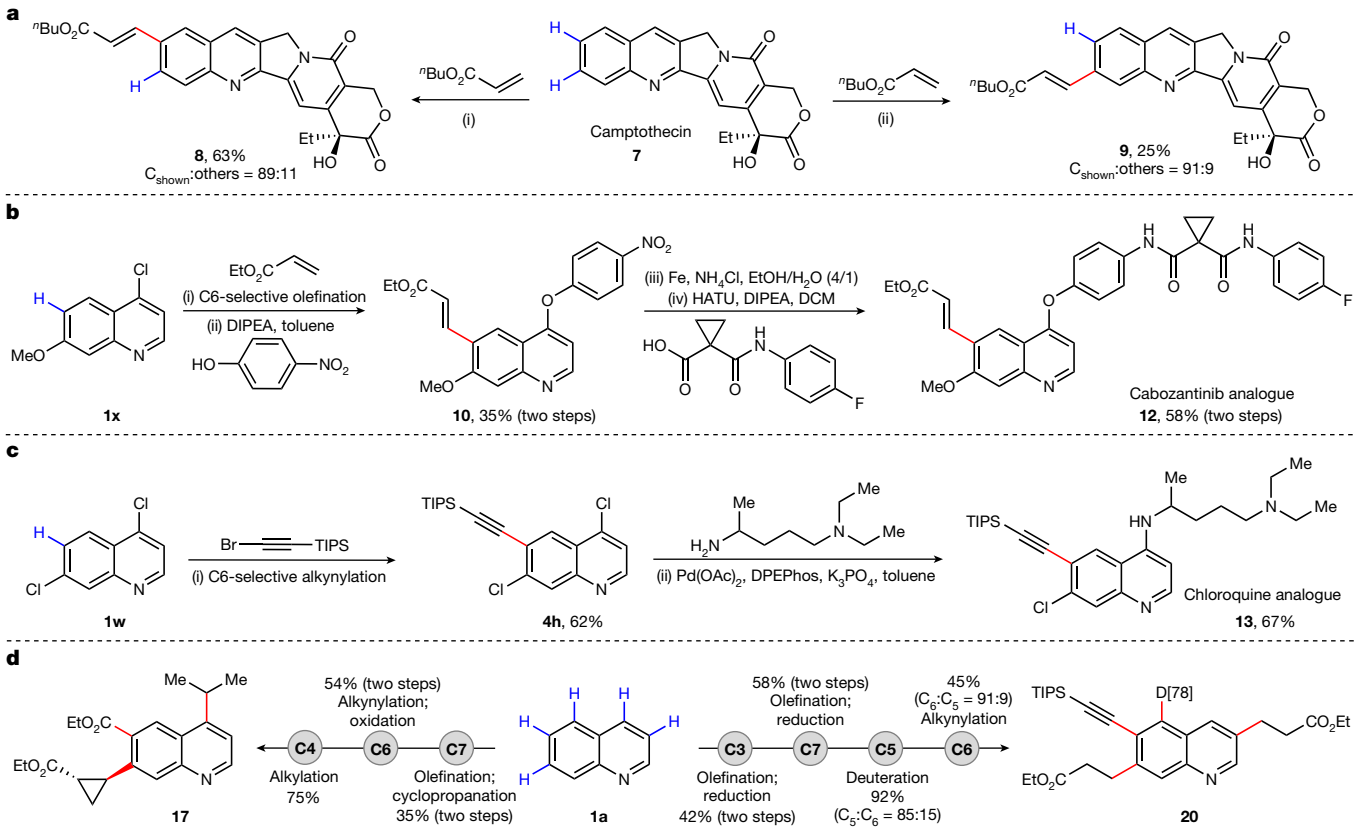

Fig. 4 | Synthetic applications. a, Late-stage remote site-selective C–H modification of camptothecin. Reaction conditions are provided in Supplementary Information Section 2.10. **b**, Synthesis of the cabozantinib analogue through C6–H olefination. **c**, Synthesis of the chloroquine analogue through C6–H alkynylation. **d**, Molecular editing of quinoline through iterative C–H activation in different orders. The reaction conditions are provided in Supplementary Information Section 2.13. Deuterium incorporation is shown in square brackets. DIPEA, N,N-diisopropylethylamine; DPEPhos, bis[(2-diphenylphosphino)phenyl] ether; HATU, 1-[bis(dimethylamino) methylene]-1H-1,2,3-triazolo[4,5-b]pyridinium 3-oxide hexafluorophosphate.

electronic preferences. A series of multiply substituted and polycyclic quinolines were also well tolerated (**2t** to **2aa**), and we were pleased to find that the reaction tolerates a variety of aza-arenes; quinoxaline (**2ab**), benzothiophene (**2ac**), phenazine (**2ad**) and thieno[2,3-b]pyridine (**2ae**) all afforded the desired products in good yields and high selectivities. Next, we examined the scope of coupling partners with unsubstituted quinoline under the standard conditions (Extended Data Fig. 1). A variety of acrylates (**2af** to **2al**), vinylamides (**2am** and **2an**), vinylsulfone (**2ao**), vinylphosphonate (**2ap**), styrenes (**2as** to **2au**) and more complex terpenoid-derived acrylate coupling partners (**2aq**, from L-menthol; **2ar**, from tetrahydrogeraniol) were well tolerated, delivering the corresponding products in good to excellent yields and selectivities.

Density functional theory (DFT) studies were conducted to understand the origin of C6 selectivity in our catalytic templates. Analysis of the concerted metalation–deprotonation (CMD) step immediately excluded a C7-selective pathway because of higher energies incurred by repulsive interactions between the template phenyl ring and ligand acetyl groups (Fig. 2c). The analysis also suggested that the initial C–H metalation was probably unselective between C5 and C6, which was supported by observing unselective substrate deuterium incorporation (Supplementary Information Section 2.14). A larger template distortion required to access the C5 position results in a lower energy barrier for the C6-selective alkene insertion step relative to C5. Therefore, a combination of a more favoured C–H activation (disfavouring C7) and alkene insertion steps (disfavouring C5) gives rise to the observed C6 selectivity for template **T12**.

The success of our C6-selective catalytic template prompted us to investigate whether C7 selectivity was also feasible through judicious spatial optimization. Our study commenced with 3-methylquinoline **1d** bearing no C–H bond at the C3, wherein an initial hit was found using a template bearing a two-carbon spacer to the directing 3-pyridyl motif (**T20**, Fig. 3a). Template rigidification (**T22** and **T24**, Fig. 3a) improved yield and selectivity, with *cis*- and *trans*-**T24** notably delivering the product **3a** in high selectivity. Systematic tuning of the template's left arm identified that a 2,6-dimethoxyphenyl motif provided markedly improved C7 yield and selectivity, with the best C7-selective template (*cis*-**T25**, Fig. 3a) affording **3a** in 67% nuclear magnetic resonance (NMR) yield with 96:4 selectivity. Using racemic *cis*-**T25** and a Ac-DL-Phe-OH ligand, a range of C3-, C4- and C2-substituted quinolines smoothly afforded the C7-olefinated products (**3a** to **3m**) in good yield and excellent selectivity (Fig. 3a). Other pharmaceutically important heterocycles (quinoxaline, benzothiophene and phenanthridine) were also compatible, generating distally olefinated products **3n** to **3p** in a site-selective manner. In addition, a diverse set of olefinic coupling partners were competent using **1d** as the substrate, successfully reacting with acrylates (**3q** to **3t**, **3x** and **3y**), vinyl sulfone (**3u**), vinyl phosphonate (**3v**) and styrene (**3w**) in moderate to good yields with excellent C7 selectivity (Extended Data Fig. 2).

However, subjecting unsubstituted quinoline **1a** with racemic *cis*-**T25** under our optimized conditions gave a disappointing 50:50 mixture of products at the C3 and C7 positions in 56% total yield (Fig. 3b). This outcome restricts the order of the iterative C–H activation sequence and affirms the initial analyses indicating the similar spatial (distance and geometry) positioning of the C3–H and C7–H bonds relative to the anchoring azine nitrogen; this is an observation supported by DFT calculations (Supplementary Fig. 12). Further inspired by the use of chiral catalysts to control site-selective modifications in chiral

polyol-containing natural products[24,25], we wondered if a matched combination of an enantiopure directing template and a chiral catalyst could distinguish between these two highly similar positions. Thus, C7 selectivity was re-evaluated against unsubstituted quinoline **1a** in the presence of enantiopure (*R,R*)- and (*S,S*)-**T25** with Ac-L-Phe-OH as the chiral ligand. We found that the use of (*S,S*)-**T25** matches the chiral ligand, providing **3z** with high C7 selectivity (C_7:C_3 = 88:12). The mismatched combination of (*R,R*)-**T25** with Ac-L-Phe-OH gave mixture products (C_7:C_3 = 50:50). Further optimization of (*S,S*)-**T25** with chiral ligands afforded **3z** in 54% yield and selectivity (C_7:C_3 = 90:10) (Fig. 3b). These results indicate that competing C–H bonds that are spatially (distance and geometrically) similar can also be distinguished through matched chirality recognition. Under the optimal conditions, C5- and C6-substituted quinolines, which gave no selectivity in the presence of racemic *cis*-**T25** and ligand, provided **3aa** to **3ad** in moderate yields and high C7 selectivities (Fig. 3b).

To rationalize the observed C7 selectivity of the chiral template (*S,S*)-**T25**, hydrogen/deuterium (H/D) exchange experiments were conducted with unsubstituted quinoline **1a**. These experiments demonstrated that deuterium incorporation at the C7 position is more favoured in the presence of the matched chiral template–ligand combination (Supplementary Information Section 2.14). As these chiral ligands are known to participate in the CMD transition state, our DFT analysis specifically focused on this crucial step with chiral template (*S,S*)-**T25** and ligands Ac-L-Phe-OH or Ac-D-Phe-OH. Despite extensive investigation, our free energy profiles obtained did not fully explain the high C7 selectivity that was observed experimentally. On the other hand, the observed C7 selectivity of 3-methylquinoline **1d** with racemic template *cis*-**T25** was fully consistent with the DFT analysis (Fig. 3c). *Cis*-**T25** gave the lowest energy transition state for all key steps at C7 compared with other positions (Supplementary Fig. 8). Further inspection revealed that increased template distortion was required to access both the C5 and C6 positions, leaving C7 as the sole favourable pathway for this template.

The scope of transformation intercepted from this catalytic directed remote C–H palladation was broadened through achieving the site-selective C–H alkynylation and allylation of aza-arenes (**4a** to **4j**, **5a** to **5h**, **6a** to **6f**, Extended Data Fig. 3), representing versatile linchpins for further diversification[28–30]. Uniformly, high site selectivity was obtained for the template-assisted C6- and C7-selective alkynylation reactions. The corresponding allylation reactions were similarly effective, giving comparatively higher reactivity, albeit with slightly reduced C6 selectivity. In all cases, a range of substitutions were tolerated, signalling the robustness of this catalytic template strategy for direct remote functionalization.

The applicability of this method in a drug discovery context was first exemplified by the divergent late-stage site-selective C–H functionalization of the anticancer natural product camptothecin[31] (Fig. 4a). Subjecting camptothecin to our optimized C6-selective template generated the new analogue **8** in 63% yield, whereas the corresponding C7-selective template generated its regioisomer **9** in 25% yield. Successful C–H editing of key pharmacophores was also demonstrated, providing new analogues of the anticancer agent cabozantinib **12** (refs. [32,33]; Fig. 4b) and the antimalarial agent chloroquine **13** (ref. [34]; Fig. 4c). Finally, we were keen to address the ultimate challenge of executing sequential site-selective late-stage 'molecular editing' in any desired order on a quinoline scaffold; its feasibility was demonstrated by successful iterative C–H activations to access products **17** and **20** bearing diverse substitutions (Fig. 4d).

In summary, a unified catalytic remote-directing template strategy enabled precise differentiation of remote and adjacent C6–H and C7–H bonds, as well as similar C3–H and C7–H bonds of a pharmaceutically relevant bicyclic aza-arene scaffold. The modularity of C6/C7 functionalization described herein, combined with previously reported methods, completes the suite of reactions required to edit all C–H bonds within bicyclic aza-arene scaffolds in different orders. Notably, the realization of C7–H selective activation over C3–H also established chiral recognition as an effective means in fine-tuning remote site selectivity between positionally similar C–H bonds, complementing previously used distance and geometric parameters in directing template design.

Online content

Any methods, additional references, Nature Research reporting summaries, source data, extended data, supplementary information, acknowledgements, peer review information; details of author contributions and competing interests; and statements of data and code availability are available at https://doi.org/10.1038/s41586-022-05175-1.

1. Wencel-Delord, J. & Glorius, F. C–H bond activation enables the rapid construction and late-stage diversification of functional molecules. *Nat. Chem.* **5**, 369–375 (2013).
2. Takagi, J., Sato, K., Hartwig, J. T., Ishiyama, T. & Miyaura, N. Iridium-catalyzed C–H coupling reaction of heteroaromatic compounds with bis(pinacolato)diboron: regioselective synthesis of heteroarylboronates. *Tetrahedron Lett.* **43**, 5649–5651 (2002).
3. Nakao, Y., Kanyiva, K. S. & Hiyama, T. A strategy for C–H activation of pyridines: direct C-2 selective alkenylation of pyridines by nickel/lewis acid catalysis. *J. Am. Chem. Soc.* **130**, 2448–2449 (2008).
4. Berman, A. M., Lewis, J. C., Bergman, R. G. & Ellman, J. A. Rh(I)-catalyzed direct arylation of pyridines and quinolines. *J. Am. Chem. Soc.* **130**, 14926–14927 (2008).
5. Nakao, Y., Yamada, Y., Kashihara, N. & Hiyama, T. Selective C-4 alkylation of pyridine by nickel/lewis acid catalysis. *J. Am. Chem. Soc.* **132**, 13666–13668 (2010).
6. Tsai, C.-C. et al. Bimetallic nickel aluminun mediated para-selective alkenylation of pyridine: direct observation of η^2,η^1-pyridine Ni(0)-Al(III) intermediates prior to C–H bond activation. *J. Am. Chem. Soc.* **132**, 11887–11889 (2010).
7. Ye, M., Gao, G.-L. & Yu, J.-Q. Ligand-promoted C-3 selective C–H olefination of pyridines with Pd catalysts. *J. Am. Chem. Soc.* **133**, 6964–6967 (2011).
8. Chen, Q., du Jourdin, X. M. & Knochel, P. Transition-metal-free BF_3-mediated regioselective direct alkylation and arylation of functionalized pyridines using Grignard or organozinc reagents. *J. Am. Chem. Soc.* **135**, 4958–4961 (2013).
9. Yamamoto, S., Saga, Y., Andou, T., Matsunaga, S. & Kanai, M. Cobalt-catalyzed C-4 selective alkylation of quinolines. *Adv. Synth. Catal.* **356**, 401–405 (2014).
10. Kwak, J., Kim, M. & Chang, S. Rh(NHC)-catalyzed direct and selective arylation of quinolines at the 8-position. *J. Am. Chem. Soc.* **133**, 3780–3783 (2011).
11. Konishi, S. et al. Site-selective C–H borylation of quinolines at the C8 position catalyzed by a silica-supported phosphane-iridium system. *Chem. Asian J.* **9**, 434–438 (2014).
12. Murai, M., Nishinaka, N. & Takai, K. Iridium-catalyzed sequential silylation and borylation of heteroarenes cased on regioselective C–H bond activation. *Angew. Chem. Int. Ed.* **57**, 5843–5847 (2018).
13. Das, S., Incarvito, C. D., Crabtree, R. H. & Brudvig, G. W. Molecular recognition in the selective oxygenation of saturated C–H bonds by a dimanganese catalyst. *Science* **312**, 1941–1943 (2006).
14. Wilson, R. M. & Danishefsky, S. J. Small molecule natural products in the discovery of therapeutic agents: the synthesis connection. *J. Org. Chem.* **71**, 8329–8351 (2006).
15. Szpilman, A. M. & Carreira, E. M. Probing the biology of natural products: molecular editing by diverted total synthesis. *Angew. Chem. Int. Ed.* **49**, 9592–9628 (2010).
16. Leow, D., Li, G., Mei, T.-S. & Yu, J.-Q. Activation of remote meta-C–H bonds assisted by an end-on template. *Nature* **486**, 518–522 (2012).
17. Kuninobu, Y., Ida, H., Nishi, M. & Kanai, M. A meta-selective C–H borylation directed by a secondary interaction between ligand and substrate. *Nat. Chem.* **7**, 712–717 (2015).
18. Davis, H. J., Mihai, M. T. & Phipps, R. J. Ion pair-directed regiocontrol in transition-metal catalysis: a meta-selective C–H borylation of aromatic quaternary ammonium salts. *J. Am. Chem. Soc.* **138**, 12759–12762 (2016).
19. Hoque, M. E., Bisht, R., Haldar, C. & Chattopadhyay, B. Noncovalent interactions in Ir-catalyzed C–H activation: L-shaped ligand for para-selective borylation of aromatic esters. *J. Am. Chem. Soc.* **139**, 7745–7748 (2017).
20. Zhang, T. et al. A directive Ni catalyst overrides conventional site selectivity in pyridine C–H alkenylation. *Nat. Chem.* **13**, 1207–1213 (2021).
21. Zhang, Z., Tanaka, K. & Yu, J.-Q. Remote site-selective C–H activation directed by a catalytic bifunctional template. *Nature* **543**, 538–542 (2017).
22. Ramakrishna, K. et al. Coordination assisted distal C–H alkylation of fused heterocycles. *Angew. Chem. Int. Ed.* **58**, 13808–13812 (2019).
23. Shi, H. et al. Differentiation and functionalization of remote C–H bonds in adjacent positions. *Nat. Chem.* **12**, 399–404 (2020).
24. Lewis, C. A. & Miller, S. J. Site-selective derivatization and remodeling of erythromycin A by using simple peptide-based chiral catalysts. *Angew. Chem. Int. Ed.* **45**, 5616–5619 (2006).
25. Tay, J.-H. et al. Regiodivergent glycosylations of 6-deoxy-erythronolide B and oleandomycin-derived macrolactones enabled by chiral acid catalysis. *J. Am. Chem. Soc.* **139**, 8570–8578 (2017).
26. Dimakos, V. & Taylor, M. S. Site-selective functionalization of hydroxyl groups in carbohydrate derivatives. *Chem. Rev.* **118**, 11457–11517 (2018).
27. Chu, L. et al. Remote meta-C–H activation using a pyridine-based template: achieving site-selectivity via the recognition of distance and geometry. *ACS Cent. Sci.* **1**, 394–399 (2015).

28. Lerchen, A. et al. Non-directed cross-dehydrogenative (hetero)arylation of allylic C(sp^3)–H bonds enabled by C–H activation. *Angew. Chem. Int. Ed.* **57**, 15248–15252 (2018).
29. Fu, L., Zhang, Z., Chen, P., Lin, Z. & Liu, G. Enantioselective copper-catalyzed alkynylation of benzylic C–H bonds via radical relay. *J. Am. Chem. Soc.* **142**, 12493–12500 (2020).
30. Porey, S. et al. Alkyne linchpin strategy for drug: pharmacophore conjugation: experimental and computational realization of a meta-selective inverse sonogashira coupling. *J. Am. Chem. Soc.* **142**, 3762–3774 (2020).
31. Pan, P. et al. Structure-based drug design and identification of H_2O-soluble and low toxic hexacyclic camptothecin derivatives with improved efficacy in cancer and lethal inflammation models in vivo. *J. Med. Chem.* **61**, 8613–8624 (2018).
32. Krajewska, J., Olczyk, T. & Jarzab, B. Cabozantinib for the treatment of progressive metastatic medullary thyroid cancer. *Expert Rev. Clin. Pharmacol.* **9**, 69–79 (2016).
33. Personeni, N., Rimassa, L., Pressiani, T., Smiroldo, V. & Santoro, A. Cabozantinib for the treatment of hepatocellular carcinoma. *Expert Rev. Anticancer Ther.* **19**, 847–855 (2019).
34. Hwang, J. Y. et al. Synthesis and evaluation of 7-substituted 4-aminoquinoline analogues for antimalarial activity. *J. Med. Chem.* **54**, 7084–7093 (2011).

Publisher's note Springer Nature remains neutral with regard to jurisdictional claims in published maps and institutional affiliations.

Springer Nature or its licensor holds exclusive rights to this article under a publishing agreement with the author(s) or other rightsholder(s); author self-archiving of the accepted manuscript version of this article is solely governed by the terms of such publishing agreement and applicable law.

© The Author(s), under exclusive licence to Springer Nature Limited 2022

Data availability

The data supporting the findings of this study are available within the paper and its Supplementary Information, and free of charge from the Cambridge Crystallographic Data Centre (https://www.ccdc.cam.ac.uk/structures) under reference numbers CCDC 2078170–2078173 and 2132680.

Acknowledgements We acknowledge The Scripps Research Institute and the National Institutes of Health (National Institute of General Medical Sciences grant no. R01 GM102265) for their financial support. Computations were performed on the Hoffman2 cluster at University of California Los Angeles (UCLA) and the Extreme Science and Engineering Discovery Environment (XSEDE), which is supported by the National Science Foundation (NSF) (grant no. OCI-1053575). We are grateful for financial support of the UCLA work from the NSF (grant no. CHE-1764328 to K.N.H.) and the NSF under the NSF Center for Selective C–H Functionalization (grant no. CHE-1700982). J. Chen, B. Sanchez and E. Sturgell are acknowledged for their assistance with liquid chromatography–mass spectrometry analysis. We thank M. Gembicky, J. Bailey and the University of California San Diego Crystallography Facility for X-ray crystallographic analysis.

Author contributions Z.F. developed the templates, optimized the conditions and investigated the substrate scope. X.C. and J.J.W. performed the DFT calculations. Z.F. and K.T. developed the template chaperones. H.S.P. and N.Y.S.L. prepared part of the substrates and reagents. K.N.H supervised the mechanistic study. J.-Q.Y., K.N.H., Z.F. and N.Y.S.L. prepared the manuscript. J.-Q.Y. directed the project.

Competing interests J.-Q.Y. and Z.F. are inventors on a patent application related to this work (US Patent application 63/334,828) filed by The Scripps Research Institute. The authors declare no other competing interests.

Additional information
Supplementary information The online version contains supplementary material available at https://doi.org/10.1038/s41586-022-05175-1.
Correspondence and requests for materials should be addressed to K. N. Houk or Jin-Quan Yu.
Peer review information Nature thanks the anonymous reviewers for their contribution to the peer review of this work.
Reprints and permissions information is available at http://www.nature.com/reprints.

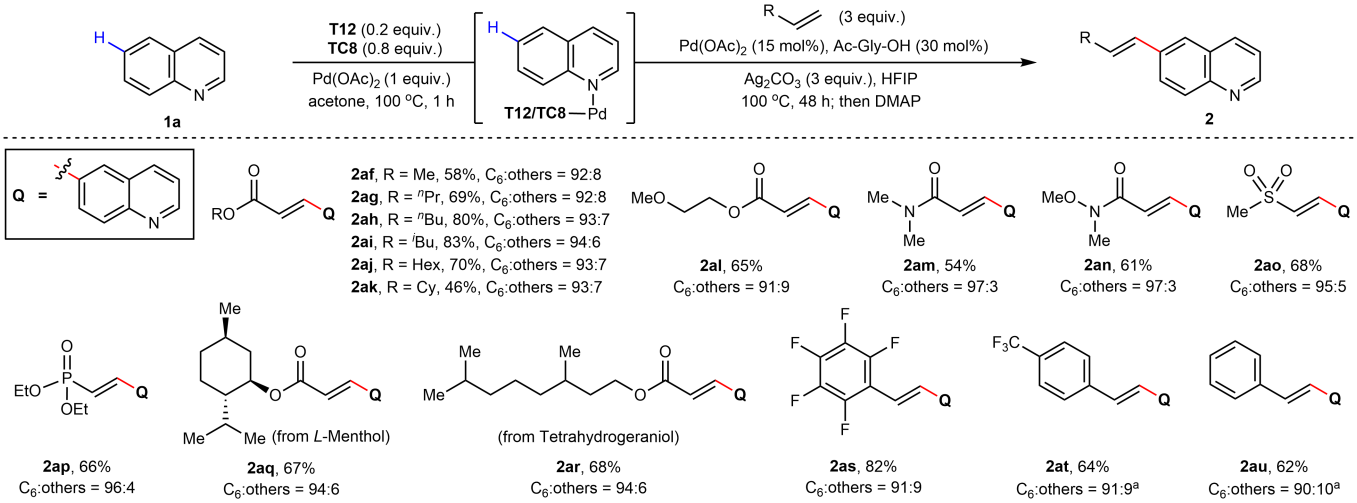

Extended Data Fig. 1 | Additional olefin scope for C6 (and related)-selective C–H olefination reactions of quinoline and other heterocycles. All yields are isolated yields. [a]Using conditions in Extended Data Fig. 3b. ^{n}Pr, n-propyl; ^{i}Bu, isobutyl; Hex, n-hexyl.

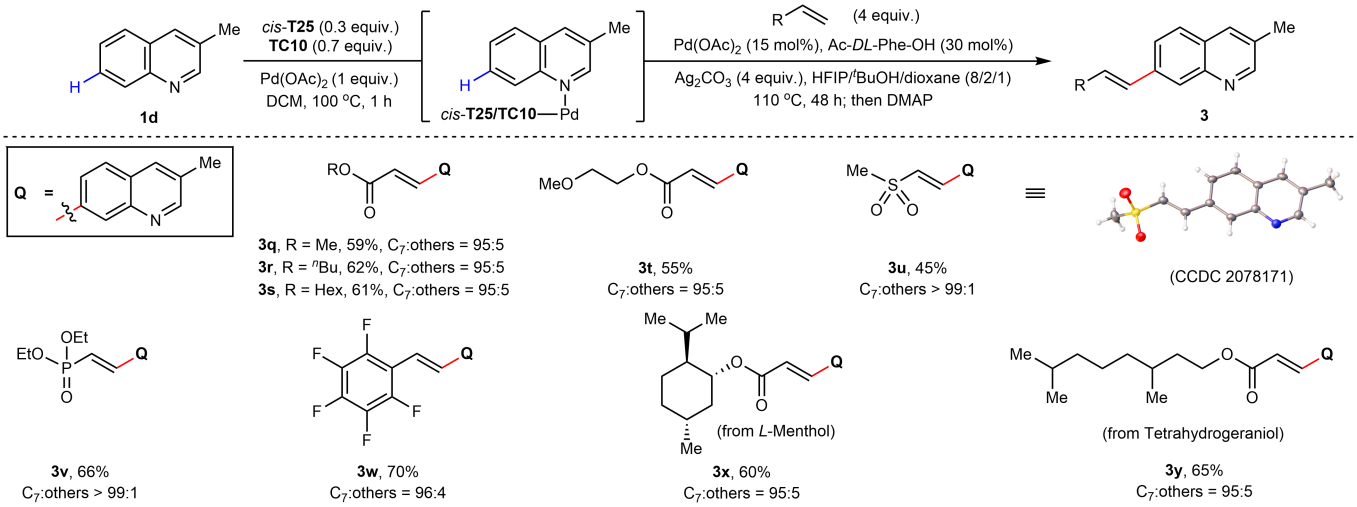

Extended Data Fig. 2 | Additional olefin scope for C7 (and related)-selective C–H olefination reactions of quinoline and other heterocycles. All yields are isolated yields.

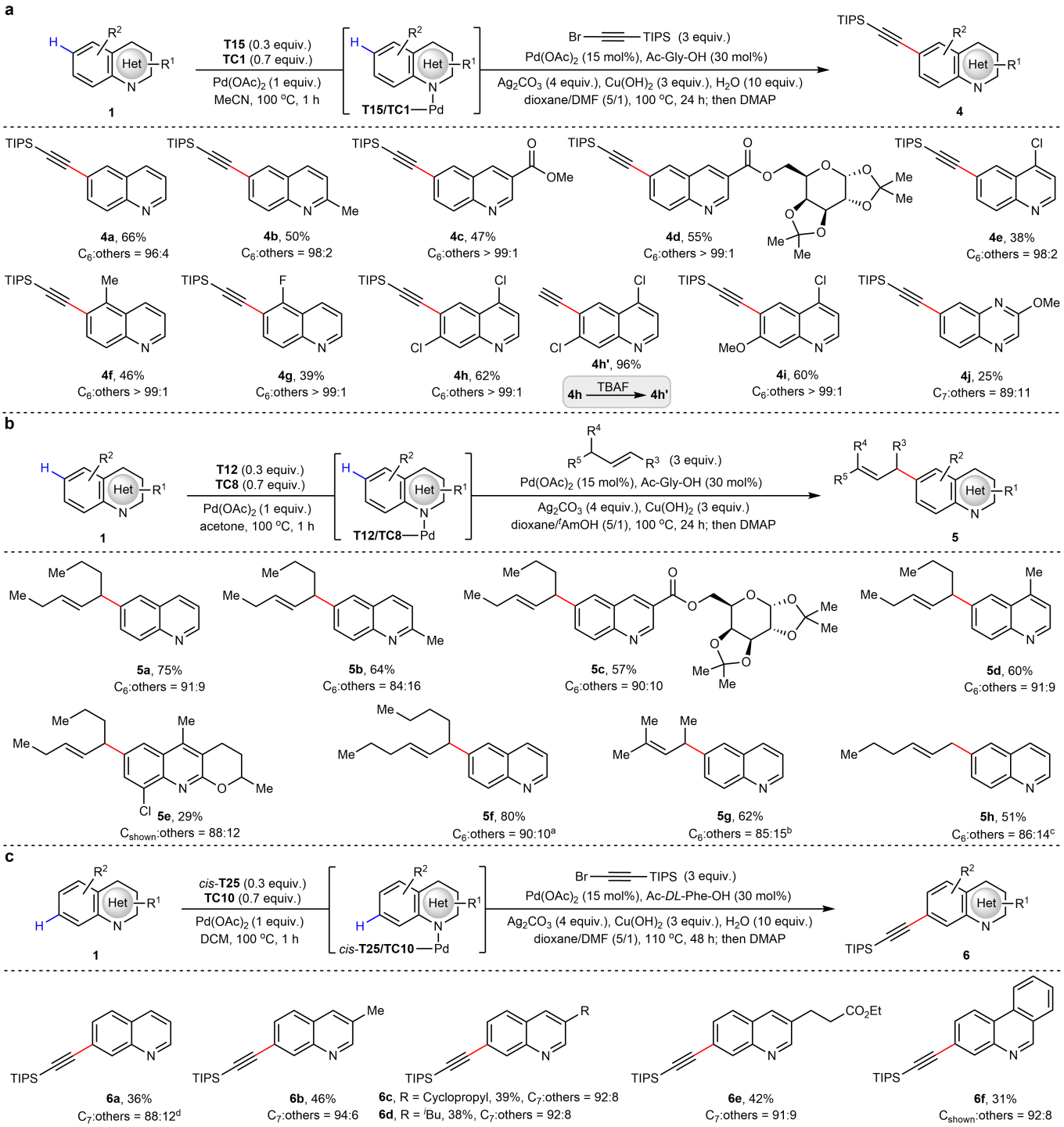

Extended Data Fig. 3 | Site-selective C–H alkynylation and allylation of aza-arenes. a, C6 (and related)-selective C–H alkynylation of aza-arenes. **b**, C6 (and related)-selective C–H allylation of aza-arenes. **c**, C7 (and related)-selective C–H alkynylation of aza-arenes. All yields are isolated yields. [a]Using *trans*-5-decene (3 equiv). [b]Using *trans*-4-methyl-2-pentene (3 equiv). [c]Using 1-hexene (3 equiv). [d]Using (*S,S*)-**T25** (0.3 equiv), $Pd(OAc)_2$ (20 mol%), Ac-*L*-Phe-OH (40 mol%), alkynylation reagent (4 equiv), 100 °C. TBAF, tetra-n-butylammonium fluoride.